Electrochemical Deposition of Mixed Ce-Al Oxide Layers on Stainless Steel and Assessment of their Corrosion-Protective Ability

DESISLAVA GUERGOVA[1], EMILIA STOYANOVA[1], IVALINA AVRAMOVA[2], DIMITAR STOYCHEV[1]*

[1] Institute of Physical Chemistry Rostislaw Kaischew, Bulgarian Academy of Sciences, Acad. G. Bonchev str., Bl. 11, 1113 Sofia, Bulgaria

[2] Institute of General and Inorganic Chemistry, Bulgarian Academy of Sciences, Acad. G.Bonchev str., Bl. 11, 1113 Sofia, Bulgaria

The corrosion protective ability of the electrodeposited mixed nanocrystalline $(CeO_2)_x(Al_2O_3)_{1-x}$ *layers has been studied in 0.1M* HNO_3 *solution as a function of the changing ratio between* CeO_2, $CeAlO_3$ *and* Al_2O_3 *on the modified SS surface. It was ascertained that the mixed layer changes substantially the character of the cathodic corrosion reaction, which leads to changes in the control of the corrosion process and stabilization of the passive state of the SS, the system* $(CeO_2)_x(Al_2O_3)_{1-x}$*/SS respectively, in case of prolonged corrosion testing.*

Keywords: electrodeposition, mixed Ce-Al oxide films on stainless steel, corrosion-protective ability

There are data in the current literature evidencing that the modification of stainless steels by addition of some lantanides improves the protective properties of the passive films on their surface [1-8]. In our previous investigations it had been established that in a corrosive medium, containing HNO_3 or H_2SO_4, for electrochemically deposited on stainless steel OC404 (SS) thin ceria or alumina layers (the systems Ce_2O_3-CeO_2/SS and Al_2O_3/SS), this effect was taking place [9-14].

These changes of the SS surface lead to significant shift in the corrosion potentials (E_{corr}) of the systems in the positive direction, decreasing their corrosion currents (j_{corr}) respectively, in different aggressive media. The established more positive potentials determine the occurrence of corrosion process of the modified SS under the conditions of stable passivity. In the cases, when the passive state of the systems is disturbed (after thermal treatment or mechanical scratch), the steel surface parts, covered with Ce_2O_3-CeO_2, begin to act as effective cathodes restoring the passive state resulting in a self-healing effect [14]. This effect is very important because the stainless steels of the type OC404 have increasing application as metallic supports of catalytically active systems in converters for neutralization of harmful exhaunst gases with high concentrations of NO_x, CO, SO_x, hydrocarbons and other environmental pollutants. It is known that under working conditions of the SS converters the formation of HNO_3 and H_2SO_4 is very probable, which could lead to their corrosion damages [15,16]. We should mention also that the active state of the active phase (Pd, Pt, etc.) in the catalytic converters strongly depends on the acid resistance of its support (Al_2O_3, CeO_2, ZrO_2, SiO_2, SiO_2-Al_2O_3, SiO_2-ZrO_2, MgO, etc.) formed on the steel substrates [17].

As we mentioned above, our previous investigations [9,18] showed that among the oxide layers studied Ce_2O_3-CeO_2 has a pronounced stabilizing effect on the passive state of steel and its corrosion resistance. This effect in case of Al_2O_3 layers is not so well expressed. At the same time more than twice-lower corrosion current is achieved in the passive region for the consecutivly deposited Al_2O_3 and Ce_2O_3-CeO_2 layers for the electrodeposited double system Ce_2O_3-CeO_2/Al_2O_3/SS. The obtained results also indicate that combinations of separate Al_2O_3 and Ce_2O_3-CeO_2 layers produce no change in the potential zones, where the steel is in its stable passive state [9].

At the same time, the data reported in [19] and [20], give evidence that:

-In case of direct electrodeposition of mixed nanocrystalline $(CeO_2)_x(Al_2O_3)_{1-x}$ $(0.1 < x < 0.8)$ films on stainless steel OC404 the XPS investigation has established that as a result of the strong interaction between CeO_2 and Al_2O_3 during the deposition process two ceria containing phases are being formed in the as-deposited layers: CeO_2 and a $CeAlO_3$-like phase;

- the formation of the $CeAlO_3$-like phase contributes to the stabilization of the textural properties of the mixed oxide layers;

-at low ceria loadings the main constituent on the covered by Ce_2O_3-CeO_2 and Al_2O_3 steel surface is mixed $CeAlO_3$ compound, while at high ceria loading the layer is constructed by CeO_2 and $CeAlO_3$ spread over the Al_2O_3 sublayer.

In the light of the above statements, the aims of the present study were formulated as follows: I - electrochemical deposition on substrate of stainless steel ÎÑ404 of model mixed oxide layers of ceria and alumina (containing Ce-Al-O bonding), for the deposition of which the ratio between the cerium and aluminium salts in the working electrolyte, respectively of cerium and aluminium containing oxide components in the electrodeposited mixed $(CeO_2)_x(Al_2O_3)_{1-x}$ layers, are varying within definite limits; II - investigation and assessment of the corrosion-protective ability of these mixed model layers in nitric acid corrosive medium as a function of the changing ratio between CeO_2, $CeAlO_3$ and Al_2O_3 on the modified steel surface.

Experimental part

All the experiments were carried out in a thermostated electrochemical glass cell. The stainless steel samples/substrate were 10 mm × 10 mm square plates of steel foil OC404 (20.0% Cr, 5.0% Al, 0.02% C, and the rest being Fe), 50 µm thick. The cathodic deposition of mixed

---

** email: stoychev@ipc.bas.bg, Phone: +359 2 720608*

$(CeO_2)_x(Al_2O_3)_{1-x}$ layers was performed in galvanostatic regime (i= 0.1 to 0.3 Adm^{-2}) and deposition time interval of 80 min. The electrolyte was prepared by addition of different contents of $AlCl_3x6H_2O$ and $CeCl_3x7H_2O$ to saturated absolute univalent alcohol until they were dissolved. The change of the content ratio between Al_2O_3 and Ce_2O_3 in the electrodeposited layers we realized by change in the ratio between concentrations (in g-ions/L) of Ce^{3+} and Al^{3+} ions in the three types of working electrolytes: Electrolyte I - $Ce^{3+} : Al^{3+}$ = 1:3 g-ions/L; Electrolyte II - $Ce^{3+} : Al^{3+}$ = 4:1 g-ions/L; Electrolyte III - $Ce^{3+} : Al^{3+}$ = 17:1 g-ions/L. The temperature of the working electrolyte was kept at a constant value of 10 C±2 in a specially constructed electrochemical cell by water-cooling circulation. The obtained mixed oxide(s) layers had a thickness ~ 4 μm. The *reference* Ce_2O_3-CeO_2 and Al_2O_3 layers were deposited electrochemically from analogous non-aqueous electrolytes containing 0.2 M $CeCl_3x7H_2O$ (Alfa Aesar) at j=0.01 Adm^{-2} for 80 min and 0.3 M $AlCl_3x6H_2O$ (Fluka Chemie AG, purum p.a.) in voltastatic regime at 6 V for 80 min, respectively.

The phase composition was characterized by X-ray diffraction (XRD) analysis using a PANalytical Empyrean system in a parallel beam geometry (parabolic mirror and parallel plate collimator) for GIXRD. X-ray diffractometer was equipped with a multichannel detector (Pixel 3D) and Cu K_α X-ray tube. The experimental conditions were: 45 kV/40 mA, $\Omega=3^{o}$, 10-95 ^{o} 2θ range, step 0.01 ^{o}, 20 s exposition.

The morphology and structure of the samples were examined by scanning electron microscopy using a JEOL JSM 6390 electron microscope (Japan) equipped with ultrahigh resolution scanning system (ASID-3D) in regimes of secondary electron image (SEI).

The influence of the chemical composition of the investigated samples (at different Ce:Al ratios) on their electrochemical/corrosion behavior was studied in a standard three-electrode thermostated cell (100 ml volume, 0.1 M HNO_3 model corrosion medium, t = 25 °C). The model potentiodynamic polarization curves for stainless steel substrates and for the oxide/SS systems in 0.1 M HNO_3 solution (p.a. Merck with distilled water) were recorded versus a counter electrode, representing a platinum plate, and a mercury/mercurous reference electrode (MSE) (Hg/Hg_2SO_4=+0.640 V vs SHE). All the potentials, listed here, are related to MSE. The anodic and cathodic potentiodynamic polarization curves were obtained using an Electrochemical Measurement System-Gamry potentiostat/galvanostat, with a potential sweeping rate of 1 mV/s. The recording of the potentiodynamic curves was carried out starting from the open circuit potential (E_{ocp}), measured in the absence of external current both in the anodic and cathodic directions. Individual samples were used for each recorded model potentiodynamic curve. The open circuit potential of the samples under investigation was determined by direct measurement of the function E_{ocp}-τ with respect to the same reference electrode after immersion in 0.1 M HNO_3 solution as it was described in [[11]. In our next experiments and discussions we accept actually that the E_{ocp} is practically equal to the stationary corrosion potential (E_{st}).

Polarization resistance (Rp) investigations were carried out using *Corrovit (TACUSSE*L electronique). All the potentials are referenced to a mercury/mercurous reference electrode (MSE). The scan range was ± 25 mV relative to corrosion potential (E_{corr}) and the scanning was carried out in the anodic direction. The initial delay interval was 30 min, and the temperature was 25 ± 0.5 °C. The specimen's area exposed to corrosion was 4 cm, and all measurements were carried out in aerated 0.1 Ì HNO_3. Stern-Geary equation gives the fundamental reason to apply this method, which is based on the fact that higher Rp value (in Ωcm^2) corresponds to higher corrosion resistance and to lower corrosion current as well, i.e. Rp ~ 1 / I_{corr} [21,22].

The chemical composition and the chemical state of the elements in case of as-deposited samples and after their immersion into corrosion medium were monitored using X-ray photoelectron spectroscopy (XPS). The XPS analyses were performed on a Kratos AXIS Supra spectrometer with a monochromatic Al X-ray source under a vacuum higher than 10^{-8} Pa at 90 degree take-off angle. Each analysis started with a survey scan from 0 to 1200 eV, pass energy of 160 eV at steps of 1 eV with 1 sweep. For the high resolution analysis the number of sweeps was increased, the pass energy was lowered down to 20 eV at steps of 100 eV. The C1s photoelectron line at 284.6 eV was used for calibration of the spectra. The surface composition was determined based on the ratio of the corresponding peak intensities, corrected with the photo ionization cross sections.

Results and discussions

GIXRD results

Figure 1 represents the GIXRD diffraction patterns of the samples with electrochemically deposited Al_2O_3, Ce_2O_3-CeO_2 and mixed thin films of $(CeO_2)_x(Al_2O_3)_{1-x}$ on SS substrates. It is seen in the figure that in addition to the highly intensive peak at $2\theta = 44.3^{o}$(pattern 1) - characteristic of the ferrite steel used as substrate - there also appear peaks, characteristic of:

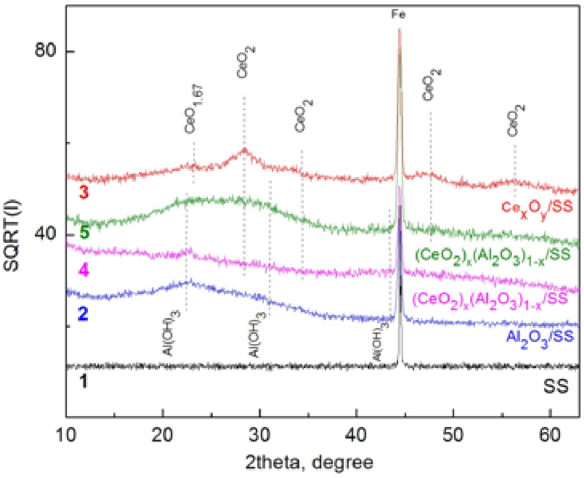

Fig. 1. GIXRD patterns of oxide films on the SS OC404 substrate - pattern 1 and as-deposited systems: pattern 2 - Al_2O_3/SS; pattern 3 - Ce_2O_3-CeO_2/SS as well as for specimens covered by mixed $(CeO_2)_x(Al_2O_3)_{1-x}$ layers, electrodeposited from electrolytes, in which the concentration ratio between Ce^{3+} and Al^{3+} ions (in g-ions/L) is 1:3 - pattern 4 and 17:1 - pattern 5.

-Aluminium hydroxide (pattern 2), when we deposited a film on the steel substrate from electrolyte, containing only 0.3 M $AlCl_3x6H_2O$. Òhere was a broad peak at 22 to 30^{o} 2θ, which can be assigned to amorphous $Al(OH)_3$;

-Ceria (pattern 3), when we deposited a film on the steel substrate from electrolyte, containing only 0.2 M $CeCl_3x7H_2O$. Ohere are peaks at 28.8, 34.2, 48.2 and 57.0, 2è corresponding to CeO_2 with fluorite structure in the bulk of the deposited layers, which can be explained by the so called *base generation mechanism* (proposed involving oxygen to produce an oxidizing agent (H_2O_2) for Ce(III) to

Ce(IV) formation) [23,24]. Confirming this mechanism are the data on the reduction of oxygen in the similar electrolytes, which show that a more preferable reaction is the incomplete reduction of oxygen leading to peroxide formation [25];

-In the case of electrodeposited mixed oxides (at ratio of Ce^{3+}:Al^{3+} = 1:3 g-ions/L (pattern 4) and = 17:1 g-ions/L (pattern 5) the broadened diffraction peaks of CeO_2 and $Al(OH)_3$ in mixed amorphous $(CeO_2)_x(Al_2O_3)_{1-x}$ films are observed at 22 to 57° 2θ. The co-deposition of CeO_2 and $Al(OH)_3$, incorporation of Al in CeO_2 respectively, centered the broad peak around 29° of 2θ, which could be assigned to amorphous Ce_2O_3 and/or intermediate mixed oxides [26,27]. According to the Y. Liu and co-authors [27] Al incorporation changes the crystalline structure of the cerium oxide layers to an *unique* amorphous or nanocrystalline structure and avoids its strong diffraction peaks, which leads to disappearance of Al in the XRD pattern of the Ce-Al-O layer. The so obtained diffraction patterns give convinicing evidence for the fact that the increase in the concentration of cerium ions in the mixed working electrolyte leads to increase in the content of cerium oxide, respectively change in the ratio between the two oxides in the deposited mixed oxide film (patterns 4 and 5), in favour of the cerium oxide component. (The latter statement, as one can see below in item 3.4., corresponds also to the data obtained by XPS analyses of the chemical composition and the state of the elements in the thin surface layer, formed from these oxides on the steel surface).

Surface morphology and microstructure of the $(CeO_2)_x(Al_2O_3)_{1-x}$ thin films

As it can be seen in Fig. 2, the change in the ratio between the concentrations of cerium and aluminium ions in the working electrolyte definitely influences the morphology and structure of the film. When this ratio is 1:3 (Fig. 2,a), the deposited mixed oxide film is characterized by relatively rough, large crystal structure, which differs from that, characteristic of the films of Al_2O_3 and CeO_2 (electrodeposited from electrolytes containing only aluminium, respectively cerium, ions) [28,29].

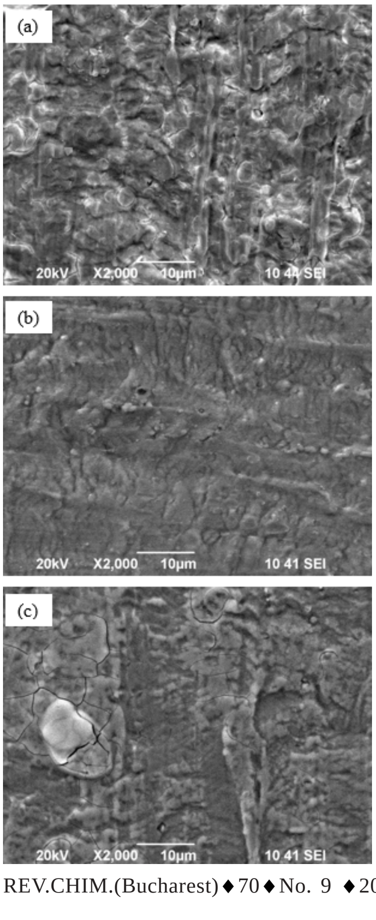

Fig. 2. SEM micrographs of mixed $(CeO_2)_x(Al_2O_3)_{1-x}$ layers electrodeposited on SS substrate from electrolytes, in which the concentration ratio between Ce^{3+} and Al^{3+} ions (in g-ions/L) is: 1:3 - 2(a); 4:1 - 2(b) and 17:1 - 2(c). Time of deposition 80 min.

Upon changing this ratio in favour of the cerium ions one observes a peculiar leveling of the surface morphology of the deposited layers, owing to several times decrease in the size of the agglomerates building up the layers (Fig. 2,b), while in case of further increase in the concenration of the cerium ions (reaching a ratio of 17:1) some cracks are appearing in them (Fig. 2,c). (*after this line can insert Figure 2*)

The registered structural changes in the studied films, corresponding directly to the changes in the ratio between the concentrations of cerium and aluminium ions in the electrolytes from which they have been prepared, respectively - changes in the concentration ratio of the two elements in the deposited mixed oxide films (see par. 3.4), can be interpreted in view of the results obtained in previous investigation [19]. In view of the XPS data established by these investigations on $(CeO_2)_x(Al_2O_3)_{1-x}$ films obtained in analogous way, the main constituent on the surface is $CeAlO_3$ intermediate oxides in case of low ceria loading sample, while at high ceria loading the film is constructed from CeO_2 and $CeAlO_3$ oxides spread over the Al_2O_3. Obviously, the formation of the $CeAlO_3$ oxide during electrodeposition of mixed $(CeO_2)_x(Al_2O_3)_{1-x}$ films at low concentrations of ceria determines the differences in their structure and morphology, in comparison with the electrodeposited layers of *pure* CeO_2 and Al_2O_3 [25,27,28]. It is logical to suppose that at high ceria concentrations in the electrodeposited mixed oxide layer, the presence of both CeO_2 and $CeAlO_3$, formed on the Al_2O_3, will lead to appearance of internal tension in the layers during their co-deposition, which results in the formation of microcracks in them (Fig.2,c).

Corrosion investigations results

Potentiodynamic investigations

Figure 3 shows that when we change the ratio between the concentrations of the ions Ce^{3+} and Al^{3+} in the working electrolyte in favour of the cerium ions - from 1:3 up to 17:1, corresponding to CeO_2 and Al_2O_3 components in the mixed protective system $(CeO_2)_x(Al_2O_3)_{1-x}$ -we find out that upon increasing this ratio in favour of cerium with more than one order of magnitude its j_{corr} is decreased (from $1.3x10^{-7}$ Acm^{-2} for the uncoated SS to $1.9x10^{-8}$ Acm^{-2} for the mixed layer obtained at ratio 17:1), accompanied by drastic (from -0.309 to +0.475 V) shift of E_{corr} of the system in positive direction, coming close to the redox potential of the ionic couple Ce^{4+}/Ce^{3+} [30,31]. In our opinion, the mixed $(CeO_2)_x(Al_2O_3)_{1-x}$ oxide layers deposited on SS act as efficient cathodic layer [11], leading to substantial change in the course of the cathodic potentiodynamic curves (Fig.3, curves 2-4). In the cases of curve 3 and especially curve 4, the strong shifting in the corrosion potential of the system in positive direction could also be associated with the occurrence of a cathodic process of reduction of the oxidative component in the surface film - CeO_2. Their presence on the surface of SS determines the occurrence of cathodic corrosion reaction, depicted as potentiodynamic cathodic curves, which intersect the anodic potentiodynamic curve for SS in the zone of potentials (~ -0.250 ÷ +0.450 V), where it is located in a state of deep passivation (Fig. 3, curve 1).

The comparison of these results with the data from the potentiodynamic model curve, obtained in the same corrosion medium on samples of pure Fe (Fig. 3, curve 5) gives us reasons, to accept that in addition to the screening protective action, the influence of the electrodeposited

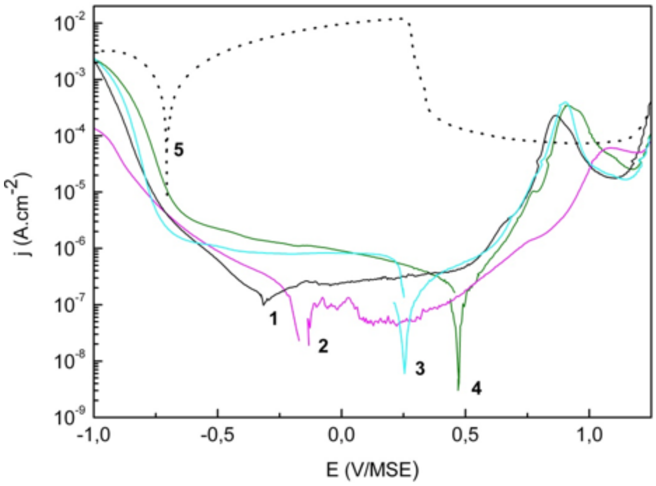

Fig. 3. Potentiodynamic E-lgj curves obtained in 0.1 M HNO_3 for: SS substrate (curve 1); the different systems mixed $(CeO_2)_x(Al_2O_3)_{1-x}$/ SS, obtained from electrolytes, in which the concentration ratio of $Ce^{3+} : Al^{3+}$ (in g-ions/L) is:1:3 (curve 2), 4:1 (curve 3) and 17:1 (curve 4). The potentiodynamic curve 5 characterizes the specimen prepared from *bare* Fe.

mixed $(CeO_2)_x(Al_2O_3)_{1-x}$ layers on the corrosion behaviour of SS could be connected also with the strong shifting of E_{corr} of these systems in positive direction, thereupon reaching the zone of deep passivation of the main (iron) component in the SS (at $E_{corr} > +0.25$ V vs MSE, Fig. 3, curve 5). Obviously when the ratio between CeO_2 and Al_2O_3 is in favour of CeO_2, this shift, respectively reaching the zone of stable passive state of the main iron component of SS, is more efficient. At the same time, what also makes impression, is that at a ratio between the concentrations of $Ce^{3+} : Al^{3+} = 1:3$ in the electrolyte (Fig.3, curve 2), whereupon the aluminium component in the mixed oxide layer is dominating, the depolarizing cathodic reaction is the process of reduction of the hydrogen ions. Obviously in this case the deposited mixed $(CeO_2)_x(Al_2O_3)_{1-x}$ film determines a specific anodic protection of the steel surface (see anodic part of the curve 2). A confirmation of this statement is the decrease in the currents of complete passivation with about an order of magnitude (Fig. 3, curves 1 and 2).

When we discuss the stabilization of the passive state of SS, protected by CeO_2, Ce_2O_3, Al_2O_3 and especially their mixed oxide layers, it is necessary to have in mind also the following fact. The established increasing protective effect upon increasing of ceria component in mixed Ce-Al-O layers is probably due to the fact that CeO_2, Ce_2O_3 and Al_2O_3 oxides have close values of the stability, since the enthalpy of their formation is respectively 1089, 1796, 1676 kJ/mol [32] on one hand, while on the other hand - the dielectric measurements have shown, that the mixed cerium-aluminium oxide has almost twice higher value of the dielectric constant in comparison with that measured with pure aluminium oxide [33].

Chronopotentiometric investigations

In confirmation of these conclusions come also the results, obtained during the study of the change in the potential upon immersion (E_1) and the changing/ establishing with the course of time of exposure E_{st} for the same systems, by plotting the chronopotentiometric E_{st}-τ curves obtained in the same corrosion medium. The data from a similar type of studies bring us closer to a considerable degree to the results from the native corrosion testings and they enable the opportunity to make a relatively fast, simple and reliable evaluation and juxtaposition with the data from the accelerated model investigations, based on the potentiodynamic curves and on the corrosion parameters, determined on their basis. The justification of such juxtaposition between the results, obtained by Å-lgj (conditions of cathodic and anodic polarization) and E_{st}-τ (conditions of self-dissilution) curves provides the electrochemical nature of conjugated occurring cathodic and anodic reactions of the corrosion process.

From the results in Fig. 4 and in Table 1 it can be seen that the deposited CeO_2, Al_2O_3 or mixed $(CeO_2)_x(Al_2O_3)_{1-x}$ layers on SS influence substantially the corrosion potential of the systems studied in 0.1 M HNO_3 solution. Thereupon the own corrosion protective influence of the individually deposited layers of Ce_2O_3-CeO_2 or Al_2O_3 is clearly expressed as well as the contribution of each one of them as component in the mixed $(CeO_2)_x(Al_2O_3)_{1-x}$ systems.

Table 1

VALUES OF THE POTENTIALS OF IMMERSION (E_1) AND THE STATIONARY POTENTIALS (E_{st}) AFTER 500 AND 1200 hours OF EXPOSURE OF THE STUDIED SYSTEMS IN 0.1 M HNO_3

Systems	E_1 (V)	E_{st} (V) after 500 h	E_{st} (V) after 1200h
SS substrate	-0.335	-0.020	-0.112
Al_2O_3/SS	-0.288	0.072	0.007
Ce_2O_3-CeO_2/SS	0.189	0.106	0.118
$(CeO_2)_x(Al_2O_3)_{1-x}$/SS $Ce^{3+} : Al^{3+} = 1:3$ g-ions/L	-0.476	0.075	0.096
$(CeO_2)_x(Al_2O_3)_{1-x}$/SS $Ce^{3+} : Al^{3+} = 17:1$ g-ions/L	-0.204	0.305	0.126

If we consider this influence with the course of time of exposure of the studied samples to the corrosive medium, we can notice four stages of development of the corrosion process. During the first stage, the duration of which is ~ 2 h (see the insert in Fig. 4), E_{st} of the sample of SS non-protected by the studied oxide layers is steadied at ~-0.4 V and it practically does not change during this time interval (curve 1). The presence of protective layer of Al_2O_3 (curve 2) or CeO_2 (curve 3) on the SS substrate until the first ~ 20 min of exposure leads to shifting of E_{st} of the respective sample up to ~+ 0.175 V, resp.+ 0.275 V. This shifting is even stronger in case of E_{st} (reaching values ~+0.480 - +0.540 V) in the cases of the samples, upon which mixed layers $(CeO_2)_x(Al_2O_3)_{1-x}$ are being deposited (curves 4-6). What makes impression is the fact that in the case of deposited mixed $(CeO_2)_x(Al_2O_3)_{1-x}$ layers the

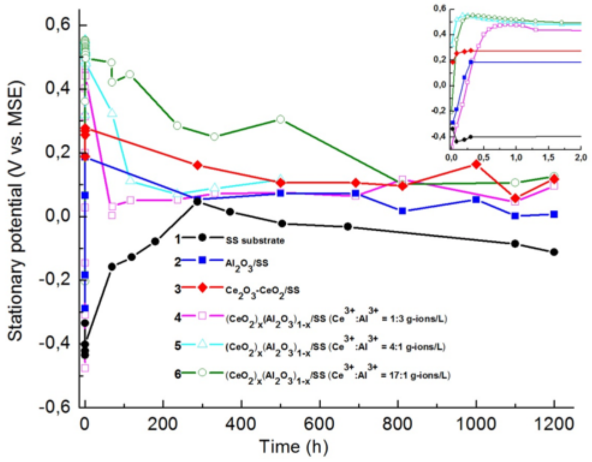

Fig. 4. Chronopotentiometric curves for the studied systems obtained in 0.1 M HNO_3 after 50 days of exposure. Insert: focus on the beginning times of exposure.

shift in E_{st} in the positive direction follows a dependence, corresponding to increased content of $(CeO_2)_x$ component in the mixed layer.

During the second stage, within the time interval ~2 - 100 h of exposure to the corrosion medium, the following changes are being registered in E_{st} of the studied samples. E_{st} of the sample of non-protected SS, as a consequence of its passivation in the corrosion medium [7,8,34,35] and formation of corrosion products is sharply shifted (up to ~ -0.130 V) in positive direction (curve 1). In the case of protected by Al_2O_3 layer (curve 2) and mixed $(CeO_2)_x(Al_2O_3)_{1-x}$ layer, in which the dominating component is Al-containig (curve 4), E_{st} is shifted strongly in negative direction - down to ~ +0.110 V, repsectively ~+0.070 V. This effect indicates lowering of the corrosion stability of the system during this period of exposure to the corrosion medium, connected most probably with corrosion attack through the available pores of the deposited layers and/or their partial dissolution in the corrosion medium. Similar, but considerably weaker effect of shifting in negative direction, reaching ~ +0.240 V, is observed for samples, protected by layer of Ce_2O_3-CeOÎ$_2$ (curve 3) or by mixed layer $(CeO_2)_x(Al_2O_3)_{1-x}$, in which the dominating component is Ce-containing (curve 5 - sample, obtained from electrolyte, in which the ratio Ce^{3+} : Al^{3+} is 4:1 g-ions/L). Practically unchanged until the 100th hour of exposure remains only the E_{st} for the system $(CeO_2)_x(Al_2O_3)_{1-x}$/SS, in which the mixed protective layer has been deposited from electrolyte, in which the ratio Ce^{3+} : Al^{3+} was maximized (17:1 g-ions/L) - curve 6.

During the third stage, within the time interval ~ 100 - 400 h of exposure to corrosive medium, the following changes in E_{st} are being registered for the studied samples. The E_{st} of the sample of non-protected SS (curve 1), as a consequence of its reactivation in the corrosive medium after the ~280th hour of the exposure (when the highest degree of passivation is reached - E_{st}= + 0.060 V), there starts shifting in the negative direction, reaching on the ~ 400th hour value for E_{st} ~ +0.020 V. In the cases of the samples, protected by layer of: Al_2O_3 (curve 2); mixed layer $(CeO_2)_x(Al_2O_3)_{1-x}$ (in which the dominating component is Al_2O_3) - curve 4 and layer of Ce_2O_3-CeO_2 (curve 3), the shift in E_{st} in negative direction on the ~ 400th h of exposure reaches a definite stationary value (respectively to ~ +0.030 V; ~ +0.080 V and ~ +0.090 V), which in the case of further exposure (until the 1200th h) practically does not change any more. The most insignificant changes in E_{st} until the 400th h of exposure are being registered for the system $(CeO_2)_x(Al_2O_3)_{1-x}$/SS, in which the mixed protective layer is deposited from electrolyte, in which the ratio between Ce^{3+} : Al^{3+} is 17:1 g-ions/L (curve 6). It is decreasing from ~ +0.470 V down to ~+0.300 V - a value which is preserved until the 550th hour of its exposure in the corrosive medium. During its further exposure - within the time interval 550 - 820 h - E_{st} for this system becomes lower ~ +0.100 V, and thereafter until the 1200th h it does not change practically, becoming steady at ~ +0.126 V.

It follows from the above represented results, that the most efficient and prolonged protection is displayed by the mixed $(CeO_2)_x(Al_2O_3)_{1-x}$ layer, which has been deposited from electrolyte, in which the ratio between Ce^{3+} : Al^{3+} is 17:1 g-ions/L, respectively the component $(CeO_2)_x$ in the mixed layer is of the greatest content (see item 3.4 XPS results). E_{st} of this system until the 500th h of exposute to 0.1 M HNO_3 solution has a value more positive than +0.250 V (Fig.4), which guarantees a stable passive state of SS. Even after the 500th hour (within the time interval 500 - 1200 h of exposure to corrosive medium), E_{st} of the mixed $(CeO_2)_x(Al_2O_3)_{1-x}$ systems (curves 4-6), as well as that of the Ce_2O_3-CeO_2 layer (curve 3), continue to be characterized by values of ~ +0.120 V stabilized in time, while E_{st} of the non-protected SS is decreased down to ~ -0.110 V, which continues to be shifting in the negative direction in the course of time.

The results discussed so far and the conclusions based on them induced carrying out some additional accelerated model testing, whereupon we recorded potentiodynamic E-lgj curves with samples of SS and samples, which showed the slightest and the strongest shifting of E_{st} in positive direction for the systems $(CeO_2)_x(Al_2O_3)_{1-x}$/SS, obtained from electrolytes, in which the ratio between Ce^{3+} : Al^{3+} is respectively 1:3 or 17:1 g-ions/L. The Å-lgj curves were obtained with samples of non-coated SS and as-deposited $(CeO_2)_x(Al_2O_3)_{1-x}$/SS systems before and after their exposure (500 and 1200 h in case of open circuit) in the working cell, charged with 0.1 Ì HNO_3 solution. The aim of these experiments was to differentiate the effect of nitric acid presence, which being an oxidative reagent can passivate the steel and contribute substantially to the shifting of E_{corr} (E_{st}) of SS, respectively of the system $(CeO_2)_x(Al_2O_3)_{1-x}$/SS, in positive direction.

It is seen in the recorded potentiodynamic curves (Fig. 5a (curve 2) and 5b (curve 4)) that upon increasing the content of the $(CeO_2)_x$ component in the mixed as-deposited $(CeO_2)_x(Al_2O_3)_{1-x}$ protective layer, which was already shown in Fig. 3, a shift in E_{corr} is observable in the positive direction, accompanied by decrease in the

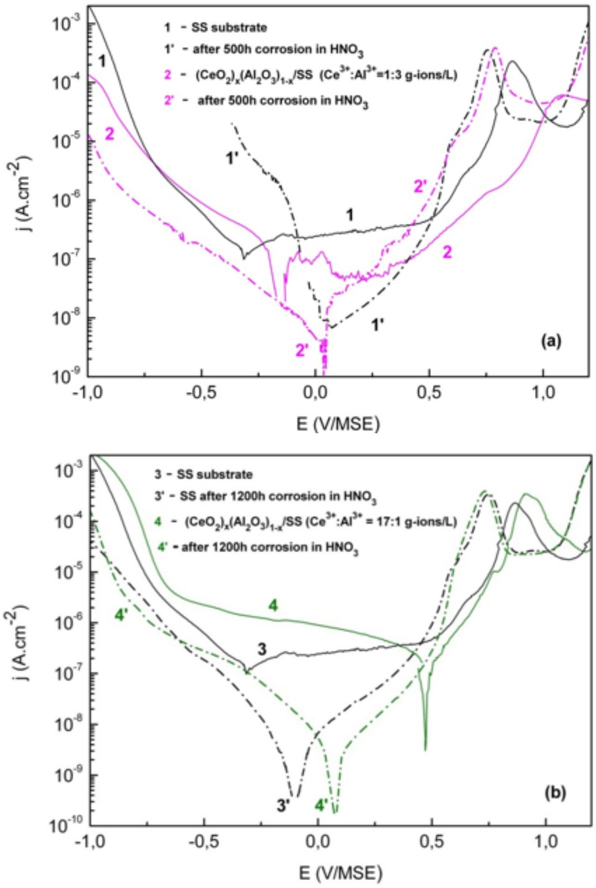

Fig. 5. Potentiodynamic E-lgj curves for the studied systems before (curves 1, 2, 3, 4) and after their long time interval of exposure in 0.1 M HNO_3 : (a) 500 h - curves 1‘, 2‘ and (b) - 1200 h - curves 3‘, 4‘. The as-deposited coating illustrated by curve 2 is obtained in electrolyte having ratio of Ce^{3+}:Al^{3+} which is 1:3 g-ions/L. The as-deposited coating illustrated by curve 4 is obtained in electrolyte with ratio Ce^{3+}:Al^{3+} of is 17:1 g-ions/L.

corrosion current. The E-lgj curves for analogous samples, taken after 500 or 1200 hours of their in 0.1 M HNO$_3$ (Fig.5a (curves 1‘,2‘) and 5b (curves 3‘,4‘) respectively), show that really for the samples having low content of the (CeO$_2$)$_x$ component in mixed as-deposited (CeO$_2$)$_x$(Al$_2$O$_3$)$_{1-x}$ protective layer (which is deposited in electrolyte having the ratio of Ce^{3+} : Al^{3+} amounting to 1:3 g-ions/L), the shifting of E$_{corr}$ for the non-coated SS and for the system (CeO$_2$)$_x$(Al$_2$O$_3$)$_{1-x}$/SS (Fig. 5a (curves 1‘ and 2‘) practically coincides (at E~ +0.050 V). The corrosion current for the coated steel, however, is with ~ 1 order of magnitude lower. In the case of samples having high content of the (CeO$_2$)$_x$ component in the mixed as-deposited (CeO$_2$)$_x$(Al$_2$O$_3$)$_{1-x}$ protective layer (which is deposited in electrolyte in which the ratio of Ce^{3+} : Al^{3+} is 17:1 g-ions/L), which have been exposed to the corrosive medium twice longer (for 1200 h), the shifting of E$_{corr}$ for the non-coated SS and for the system (CeO$_2$)$_x$(Al$_2$O$_3$)$_{1-x}$/SS (Fig. 5b (curves 3 and 4) are differing with ~0.200 V. Thereupon the corrosion current for this system is with one more order of magnitude (10 x10^{-10}) lower. (before this line can insert Figure 5)

Polarization resistance (Rp) investigations

The results, obtained in the course of this investigation, are shown in Fig. 6. The course of changes in the values of the polarization resistance (Rp, MΩcm^2) is represented, measured with steel substrate prior to and after the deposition of mixed (CeO$_2$)x(Al$_2$O$_3$)$_{1-x}$ layers on it, as well as for the separate *pure* Al$_2$O$_3$ and Al$_2$O$_3$-CeO$_2$ layers, at room temperature (~ 25^{o}C), after long time interval (500 h) of exposure in 0.1 M HNO$_3$ solution.

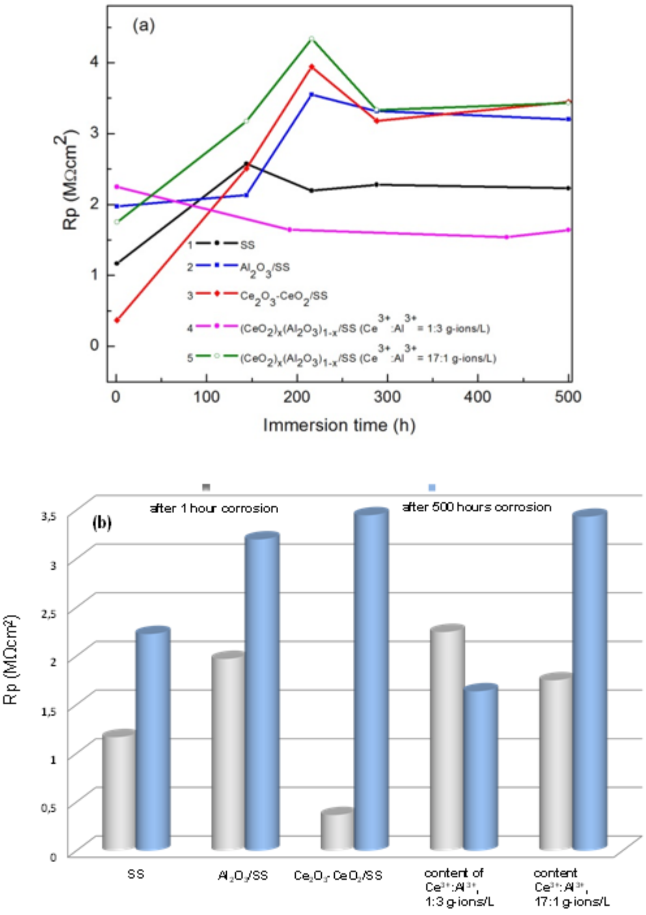

Fig. 6. The dependence “Rp vs time interval of exposure” for the studied systems in 0.1 M HNO$_3$ (a). The values of Rp after initial (1 h – white columns) and final (500 h - blue columns) time interval of exposure (b).

As it has already been ascertained and commented on by C. O’Laoire et al. [36] during exposure of stainless steels in solutions of nitric acid, at the initial moments of exposure the surface is being enriched in chromium (due to preferential dissolution of iron oxide). As a result of this the Cr$_2$O$_3$ layers being formed, is characterized by inherent corrosion resistance, low ion/electron diffusivities, and low electrical conductivity, which determine the increase in Rp of of the steel. In the case of the steel, studied by us, (Fig.6, curve 1) this process is obviously occurring until about the 140-th hour of exposure and thereafter the composition of the passive film on the surface is stabilized. Thereupon the ratio Cr/Fe in it is changed in favour of chromium as this has been shown in ref. [9] As consequence of these transformations on the steel surface its Rp is increased more than twice (starting from ~ 1.1 up to ~ 2.4 MΩcm^2).

The alterations of Rp of the steel, when layers of separate *pure* Al$_2$O$_3$ or Ce$_2$O$_3$-CeO$_2$ layers have been deposited upon it, are illustrated by the curves 2 and 3 in Fig. 6. What makes impression in these systems, is the strongly distinguished influence with respect to the changes of Rp of Al$_2$O$_3$/SS and Ce$_2$O$_3$-CeO$_2$/SS in the course of their exposure to the corrosion medium. The Al$_2$O$_3$ layers determine gradual increase in Rp of SS since the starting moment of exposure during the interval until ~ the 140-th hour. Thereafter it is becoming sharply increased until the ~ 220-th hour, and then it is decreasing (until ~ the 280-th hour). After that moment again it is slightly enhanced until ~ the 500-th hour (curve 2). The layers of Ce$_2$O$_3$-CeO$_2$, exert a negative effect during a relatively long time interval - until ~ the 140-th hour, causing a several times decrease in Rp of SS, of the system Ce$_2$O$_3$-CeO$_2$/SS, respectively. Within the interval of 210 - 280 h Rp is decreasing substantially, while after the 280-th hour it starts again slowly to increase (curve 3). It should be noted, however, that after the ~ 150-th hour of exposure the deposited Al$_2$O$_3$ and Ce$_2$O$_3$-CeO$_2$ films, within the entire studied time interval, determine the enhancement of Rp of the steel with more than ~ 50 %.

The deposition of mixed (CeO$_2$)$_x$(Al$_2$O$_3$)$_{1-x}$ layers on SS leads to a specific change in the course of variation of Rp of the steel (Fig. 6, curves 4 and 5), depending on the ratio between the aluminium-oxide and cerium-oxide component in the mixed Ce- Al oxide film. The change in to the course of curves 4 and 5 shows that when the aluminium-containing component is dominating in the mixed oxide film (curve 4), the Rp value of the steel in the time interval of exposure to the corrosion medium until the ~ 35-th hour is the highest among all the studied systems. With the course of time of exposure this Rp is gradually decreasing, reaching after the 85-th hour of immersion in to the corrosion medium the value of Rp characteristic for non-coated SS, while further during the exposure it gradually becomes lower and it is fixed at ~ 1.6 MΩcm^2 after the 180-th hour. When the cerium-oxide component is dominating in the mixed oxide film (curve 5), Rp of the steel (the system (CeO$_2$)$_x$(Al$_2$O$_3$)$_{1-x}$/SS, respectively) at the initial moments of the exposure (until ~ 35-th hour) it is lower in comparison with the mixed oxide system, in which the aluminium oxide component is dominant. Upon prolongation of the time interval of the exposure one can register a steep increase in Rp up to ~ 4.3 MÙcm^2 (on the 220-th hour), and thereafter it begins to decline. After reaching the 280-th hour again a gradual increase in Rp is observed.

The registered changes in Rp, in the course of exposure to the corrosive medium, in the cases when the investigated oxide films have been deposited on the surface of SS, could be attributed to the occurring substantial changes in the chemical composition of the surface layer of steel (the results of these studies are represented below see paragraph *3.4*). It follows on the basis of the results, represented in Fig. 6, that until about the 35-th hour of exposure to nitric acid corrosive medium the polarization, respectively the corrosion resistance of the system Al_2O_3/SS is manifested to a greatest extent, while that for the system Ce_2O_3- CeO_2/SS is lower even than the Rp of SS. This is changed after the 150-th hour of exposure, when R_p of the system Ce_2O_3-CeO_2/SS exceeds Rp of SS, while at the 220-th hour it reaches its highest value (~3.8M Ωcm^2). In the cases of mixed Ce-Àl oxide layers, in which the aluminium oxide component is the dominant one, in the course of the exposure Rp, it is continuously decreasing although quite gradually and after the ~ 80-th hour it becomes lower than that of the SS non-protected with oxide layers, while after the 200-th hour it reaches steady state at value (Rp ~ 1.6 $M\Omega cm^2$) lower than those for SS at same time intervals of exposure to the corrosive medium. The most favourable effect in this respect - maintaining high value of Rp, the corrosion-protective ability respectively, within the entire time interval of exposure to the corrosive medium is manifested by the mixed $(CeO_2)_x(Al_2O_3)_{1-x}$ layers, in which the dominating component is cerium oxide. When one deposits these layers on SS even from the starting moments of the exposure the system $(CeO_2)_x(Al_2O_3)_{1-x}$/SS is characterized by high values of Rp (~ 1.7 $M\Omega cm^2$), which reach their maximal value (~ 4.3 $M\Omega cm^2$) on the ~ 215-th hour of the exposure. The character of the changes in Rp for the studied systems during the exposure to the corrosive medium, unambiguously shows that the mixed Ce-Al oxide layers, in which the cerium oxide is dominant, have the most favourable corrosion-protection role, acting optimally within the entire time interval of exposure to the corrosive medium (Fig.6 a,b).

XPS results

The changes in the surface concentrations and states of the constituent elements of the electrodeposited on SS mixed Al-Ce oxide layers, depending on the concentration ratio of Al^{3+} and Ce^{3+} ions in the working electrolyte, have been investigated by XPS method. The Al2p and O1s as well as Ce3d photoelectron lines give information of existing surface states for the studied system in this case.

In the binding energy region of Al2p line we detect two photoelectron lines for the studied systems. The binding energy separation between them is equal to 3 eV (Fig. 7a). The low binding energy photoelectron lines for all investigated layers are situated respectively at 74.5 eV (for these electrodeposited from Electrolyte I), 74.9 eV (for these electrodeposited from Electrolyte II) and 75.2 eV(for these electrodeposited from Electrolyte III) and they are associated with the formation of mixed Ce-O-Al bonds. The second peak, which is situated at around 77.5 eV, belongs to the Al-O in aluminium oxide. According to the authors in [20] the cerium amount can rule the conductivity of the deposited films and this leads to the observed separation between the peaks in Al2p region in the present case, despite the applied charge neutralization during XPS analysis. It is interesting to point out that the observed peak positions are lower than the one for the same single aluminium oxide layers electrodeposited on SS substrate from non-aqueous electrolyte containing only 0.3 M $AlCl_3x6H_2O$ [37]. The reason for this is that in this case oxygen will receive in the -Ce-O-Al-environment higher electron density from Ce than from Al, due to the smaller electronegativity of Ce with respect to Al. In other words, -O-Al-bond are in -Ce-O-Al-binding configuration less ionic (or more covalent) than in the stoichiometric -Al-O-Al-matrix [38].

The O1s photoelectron peaks are quite wider than usual, which confirmed the existence of different bonds on the surface of deposited oxide system (Fig.7b). The lower binding energy peaks at 530.5 eV belong to Ce-O-Al type

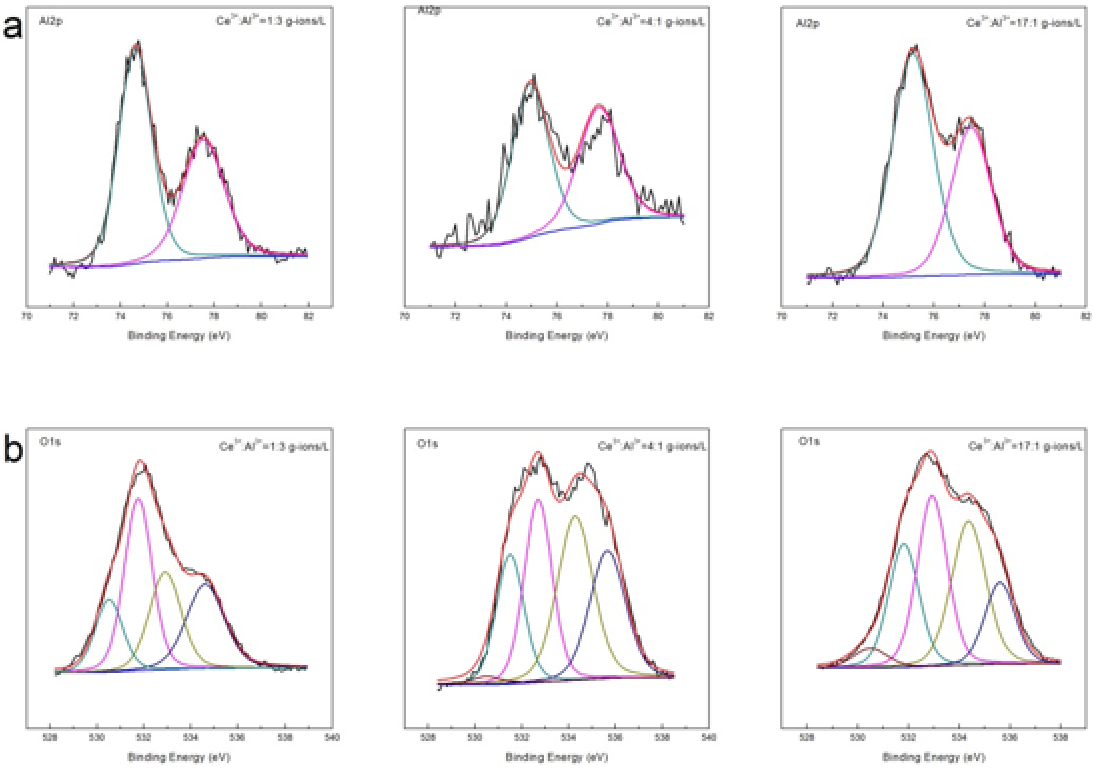

Fig. 7. XPS Al2p (a) and O1s (b) core level spectra for SS specimen, covered by mixed $(CeO_2)_x(Al_2O_3)_{1-x}$ layers, electrodeposited from electrolytes in which the concentration ratio varies.

of bond. The next two peaks are at 531.7 eV and 532.5 eV attributed to the Al-O and Al-OH bonds, respectively. The presence of another peak higher than 533 eV could be due to the existence of some water on the surface, since the deposited oxides were not subjected to any thermal treatments.

Ce3d spectra for all investigated deposited mixed oxides are typical of Ce_2O_3 and they consist of a consequence of two doublet features (Fig. 8). It is reasonable to assume that Ce^{3+} in Ce-aluminate possesses a pure $3d^{10}4f^1$ initial state configuration and after core-hole formation in the XPS Ce3d spectrum, the final state is a mixture of $3d^9 4f^2 V^{n-1}$ and $3d^9 4f^1 V^n$ configurations according to Burroughs et all [39]. Moreover a poorly expressed peak is expressed at about 916.8 eV, typical of the presence of cerium in state Ce^{4+} (CeO_2) on the surface of the studied samples. Previouslly [33] by in situ XPS studies during co-evapîration of CeO_2 and Al_2O_3 it was demonstrated that the chemical mixing of ceria and alumina is possible even at room temperature. The achievable Ce:Al ratio is only 0.02 and any higher ceria content resulted in the segregation of unmixed ceria oxide. So in this respect we can conclude that in all investigated by us samples Ce-aluminate is formed, accompanied by formation of aluminum and cerium oxides. The XPS in depth profile for the sample (not presented here), deposited from electrolyte in which the Ce^{3+} : Al^{3+} = 17:1 g-ions/L confirmed this observation. Those studies are in good agreement with findings from the XRD results (Fig. 1, pattern 5).

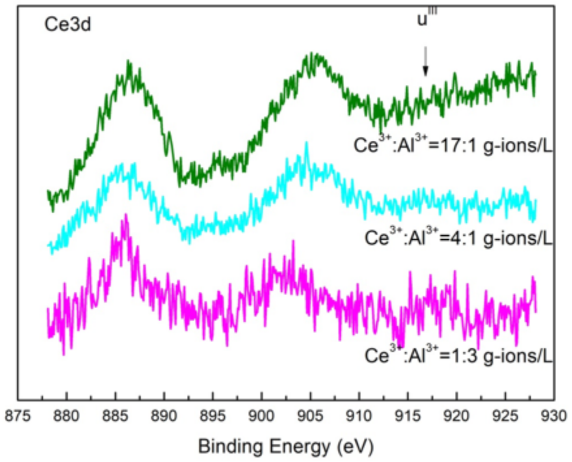

Fig. 8. XPS Ce3d core level spectra of SS specimen covered by mixed $(CeO_2)_x(Al_2O_3)_{1-x}$ layers, electrodeposited from electrolytes, in which the concentration ratio varies.

The X-ray photoelectron spectroscopy measurements were repeated with the same samples after 500 h exposure in to 0.1 M HNO_3 (Fig.9). We were focused on following the occurring changes in Al2p, O1s, Ce3d photoelectron lines mainly, nevertheless on the surface have been detected Cr, Fe and N as a result of the corrosion processes occurred.

In the Al2p region two peaks are observed. The highly intensive peaks are situated analogous to the as-deposited systems - respectively at 74.5 eV, 74.9 eV and 75.2 eV associated with the formation of mixed Ce-O-Al bonds. The other peak that appeared is evidence for the appearance of pure Al on the sample surfaces as a result of corrosion. In the O1s region no visible changes were detected. The 500 h exposure of samples into HNO_3 solutions influenced the detected amount of cerium on their surfaces. There is presence of cerium in Ce^{3+} state

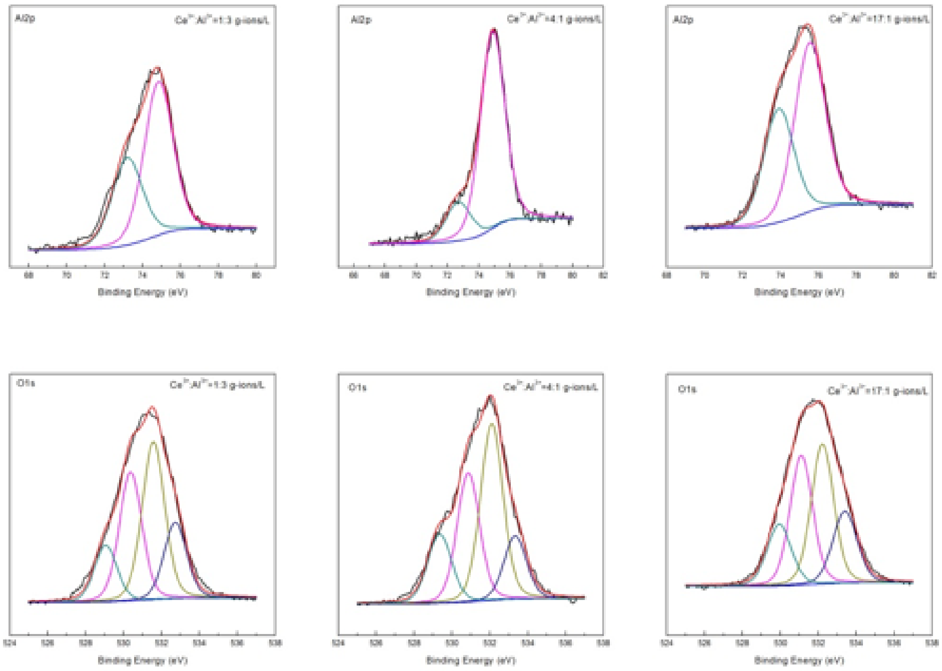

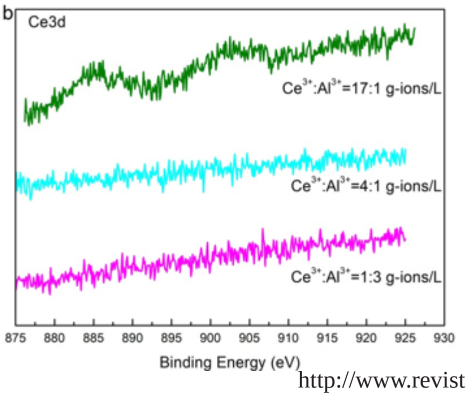

Fig. 9. Al2p and O1s (a) and Ce3d (b) core level spectra of SS specimen, covered by mixed $(CeO_2)_x(Al_2O_3)_{1-x}$ layers, electrodeposited from electrolytes in which the concentration ratio varies, after 500 h exposure in 0.1 M HNO_3 solution.

only for the sample mixed $(CeO_2)_x(Al_2O_3)_{1-x}$ layer, which is deposited from electrolyte characterized by ratio of Ce^{3+} : Al^{3+} = 17:1 g-ions/L. For the other two samples the cerium amount is less than the detectable edge, which corresponds to the data showed in Fig. 4 and already commented on.

Conclusions

The established difference in the nature, respectively in the chemical bond strength between the oxygen and the aluminium in the electrochemically obtained -Ce-O-Al- binding configuration in comparison with the stoichiometric -Al-O-Al-matrix gives us the reason to suppose that the processes of electrodeposition of mixed Ce-Al oxide layers are associated with the formation of mixed Ce-O-Al bonds. The total composition of the obtained films can be described by the formula $(CeO_2)_x(Al_2O_3)_{1-x}$, whereupon the value of **x** depends on the ratio between the concentrations of Al^{3+} and Ce^{3+} ions in the working electrolyte.

The obtained results on the better protective ability of mixed $(CeO_2)_x(Al_2O_3)_{1-x}$ layers, in comparison with the electrodeposited *pure* Al_2O_3 or Ce_2O_3-CeO_2 layers, which is enhanced with the increase in the concentration of the cerium oxide component in them. Besides this, it has also been established that with the increase of the content of cerium containing oxide component in these layers, with more than one order of magnitude the j_{corr} of the system $(CeO_2)_x(Al_2O_3)_{1-x}$/SS is decreased. These effects are connected with a drastic change of Rp, increase in passivity respectively, of the studied systems and shifting (with ~785 mV) of its E_{corr} in positive direction, approaching the redox potential of the ionic couple Ce^{4+}/Ce^{3+}. The latter fact leads to the appearance of $(CeO_2)_x(Al_2O_3)_{1-x}$ as effective cathodic layer, determining a change in the nature of the occurring cathodic and anodic processes, characterizing the corrosion of the system $(CeO_2)_x(Al_2O_3)_{1-x}$/SS.

Acknowledgement: The authors gratefully acknowledge the financial support by NSF BG Contract T 02/22.

References

1.BERNAL S., BOTANA F.J., CALVINO J.J.,MARCOS M., PEREZ-OMIL J.A., VIDAL H., J. Alloys Compd., 225, 1995, p. 6382.
2. HUSSEY R.J., GRAHAM M.J., Oxid. Met., 45, 1996, p. 349
3.MANSFELD F., BRESLIN C.B., PARDO A., PEREZ F.J., Surf. Coat. Technol., **90**, 1997, p. 224
4.MONTEMOR M.F., SIMONES A.M., FERREIRA M.G.S., Progress Org. Coat., **44**, 2002, p. 111
5.ABREU C.M., CRISTOBAL M.J., NOVOA X.R., PENA G., PEREZ M.C., RODRIGUEZ R.J., Surf. Coat. Technol., **158-159**, 2002, p. 582
6.ARENAS M.A., DAMBORENEA J.J., Electrochim. Acta, **48**, 2003, p. 3693
7.FAUVET P., BALBAUD F., ROBIN R., TRAN Q.-T., MUGNIER A., ESPINOUX D., J. Nucl. Mat., **375**, 2008, p. 52
8.KAIN V., KHAN S., REDDY A.V.R., WATTAL P.K., Advanced Materials Research, **794**, 2013, p. 517
9.STOYANOVA E., NIKOLOVA D., STOYCHEV D., STEFANOV P., MARINOVA T., Corr. Sci., **48**, 2006, p. 4037
10.GUERGOVA D., STOYANOVA E., STOYCHEV D., ATANASOVA G., AVRAMOVA I., STEFANOV P., Bulg. Chem. Commun., **40**, 2008, p. 227
11.STOYANOVA E., GUERGOVA D., STOYCHEV D., AVRAMOVA I., STEFANOV P., Electrochim. Acta., **55**, 2010, p. 1725
12.GUERGOVA D., STOYANOVA E., STOYCHEV D., AVRAMOVA I., ATANASOVA G., STEFANOV P., Bulg. Chem. Commun., **43**, 2011, p. 150
13.GUERGOVA D., STOYANOVA E., STOYCHEV D., AVRAMOVA I., STEFANOV P., Open Chem. Phys. J., 2012, p. 8
14.GUERGOVA D., STOYANOVA E., STOYCHEV D., AVRAMOVA I., STEFANOV P., J. Rare Earths, **33**, 2015, p. 1212
15. NONNENMANN M., Automobiltechnische Zeitschrift, **91**, 1989, p. 185
16. LOX E.S.J., ENGLER B. H., Handbook of Heterogeneous Catalysis, Wiley-VCH, **4**, 1997, p. 1559
17. YAZAWA Y., YOSHIDA H., TAKAGI N., KOMAI Sh., SATSUMA A., HATTORI T., J. Catal., **187**, 1999, p. 15
18. STOYCHEV D., J. Solid State Electrochem., **17**, 2013, p. 497
19. AVRAMOVA I., STEFANOV P., NICOLOVA D., STOYCHEV D., MARINOVA Ts., Comp. Sci. and Techn., **65**, 2005, p. 1663
20. AVRAMOVA I., SUZER S., GUERGOVA D., STOYCHEV D., STEFANOV P., Thin Solid Films, **536**, 2013, p. 63
21. STERN M., GEARY A.L., J. Electrochem. Soc., **104**, 1957, p. 56
22. SKOLD R.V., LARSON T.H.E., Corrosion, **13**, 1957, p. 69
23. ALDYKIEWICZ JR A.J., DAVENPORT A.J., ISAACS H.S., J. of the Electrochem. Soc., **143**, 1996, p.147
24. GOLDEN T.D., SHANG Y., WANG Qi, ZHOU T., Chapter 4 in the Book Advanced Ceramic Processing, INTECH 2015
25. VALOV I., GUERGOVA D.,STOYCHEV D., Chapter 17, Proceedings of the NATO Advanced Study Institute on Nanotechnological Basis for Advanced Sensors, Springer, The Netherlands 2011
26. ERSHOV S., DRUAT M.-E., POELMAN M., COSSEMENT D., SBYDERS R., OLIVIER M.-G., Corros. Sci., **75**, 2013, p. 158
27.LIU Y., HUANG J., CLAYPOOL J., O'KEEFE M.J., J. Electrochem.Soc., **163**, 2016, C198.
28.STOYCHEV D., STEFANOV P., NIKOLOVA D., ALEKSANDROVA A., ATANASOVA G., MARINOVA Ts., Surf. Coat. Technol., **180-181**, 2004, p. 441
29.NIKOLOVA D., STOYANOVA E., STOYCHEV D., STEFANOV P., MARINOVA T., Surf. Coat. Technol., **201**, 2006, p. 1559
30.HAYES S.A., YU P., O'KEEFE T.J., O'KEEFE M.J., STOFFER J.O., J. Electrochem. Soc., **149**, 2002, C623
31.YU P., HAYES S.A., O'KEEFE T.J., O'KEEFE M.J., STOFFER J.O., J. Electrochem. Soc., **153**, 2006, C74
32.LIDE DAVID R. (Eds), CRC Handbook of Chemistry and Physics, CRC Press, Boca Raton, FL 2005
33.SOHAL R., LUPINA G., SEIFARTH O., ZAUMSEIL P., WALCZYK C., SCHROEDER T., Surf. Sci., **604**, 2010, p. 276
34.TOMASHOV N.D., CHERNOVA G.P., Passivity and Metals Corrosion (in Russian), Publ. House Nauka, Moscow 1965
35.HANNANI A., KERMICHE F., POURBAIX A., BELMOKRE K., Trans IMF, **75**, 1997, p. 7
36.O'LAOIRE C., TIMMINS B., KREMER L., HOLMES J. D., MORRIS M. A., Anal. Letters, 39, 2006, p. 2255
37.STEFANOV P., STOYCHEV D., ALEKSANDROVA A., NICOLOVA D., ATANASOVA G., MARINOVA Ts., Appl. Surf. Sci., **235**, 2004, p. 80
38.SCHROEDER T., LUPINA G., SOHAL R., LIPPERT G., WENGER Ch., SEIFARTH O., TALLARIDA M., SCHMEISSER D., J. Appl. Phys., **102**, 2007, p. 014103
39.BURROUGHS P., HAMNETT A., ORCHRD A.F., THORNTON G., J. Chem. Soc., Dalton Trans., **17**, 1976, p. 1686

Manuscript received: 30.03.2018